15TH IEA HEAT PUMP CONFERENCE
MAY 26–29, 2026 | HOFBURG VIENNA 2026
DECARBONISATION THROUGH INNOVATION

Thermodynamic analysis of an absorption refrigeration cycle operating with the working fluid pair (CO_2+ethyl-lactate)

Alaa HAJLAOUI[a], Laurence RODIER[a], Amin ALTAMIRANO[b], Yohann COULIER[a,*]

[a]Université Clermont Auvergne, ICCF, CNRS, Clermont Auvergne INP Clermont-Ferrand, F-63000, France
[b]Lafset, Conservatoire national des arts et métiers Paris, F-75003 Paris, France

Abstract

With the increasing energy demand for cooling and in the search for alternatives to compression refrigeration machines, vapor absorption refrigeration technology is emerging as a promising solution. However, the traditional working fluids used in these machines (based on H_2O and NH_3 as refrigerants) present some disadvantages such as corrosion, low compactness, toxicity, and crystallization risks. To overcome these disadvantages, this study considers using carbon dioxide (CO_2) as refrigerant combined with a bio-based solvent, namely ethyl lactate (E-LAC). Indeed, based on new experimental heat of mixing data and considering the available literature data, ethyl lactate was identified as an interesting absorbent for CO_2. The experimental data obtained for the (CO_2–E-LAC) mixture, combined with those from the literature, were used to develop an appropriate thermodynamic model to finally assess, by calculation the performance of a single-stage absorption chiller with this working fluid pair.

Selection and/or peer-review under the responsibility of the organizers of the 15th IEA Heat Pump Conference 2026.

Keywords: Vapor Absorption Refrigeration; Carbon Dioxid; Biobased Solvent; Thermodynamic.

1. Introduction

Vapor-absorption refrigeration (VAR) technology uses thermal energy as main driving source. Therefore, waste heat recovered from industrial processes or heat supplied by renewable sources (e.g., solar and geothermal energy) can be used to operate these refrigeration systems. Furthermore, VAR cycle uses natural working fluids (WFs). Commonly used WFs in VAR cycle are binary mixtures containing a refrigerant and an absorbent and the energy performance of these cycles is critically dependent on their thermophysical properties [1]. The most widely used working fluid mixtures are water-lithium bromide (H_2O–LiBr) for positive cooling applications and ammonia-water (NH_3–H_2O) for negative cooling [1]. Despite their noteworthy thermodynamic properties, these WFs exhibit specific drawbacks such as toxicity, corrosion or solution crystallization which prevent wider use. Despite intensive research carried out either to solve issues linked to the use of (NH_3–H_2O) and (H_2O–LiBr) WFs pairs or to propose new working fluids, the VAR technology has known a very limited expansion. Hence searching for an environmentally friendly and efficient cycle using a non-toxic, non-corrosive working fluid has become of great importance. Recently, Coulier *et al.* [2] proposed to use carbon dioxide (CO_2) refrigerant with an absorbent from the biomass, namely a biobased solvent (BBS). The authors presented a methodology for preselecting the BBS based primarily on CO_2 solubility in BBS criteria. Inspired by this work and in line with the same approach, ethyl lactate (E-LAC) appears to be a relevant candidate. This bio-based solvent is attracting growing interest as a sustainable alternative to conventional

* Corresponding author. *E-mail address:* yohann.coulier@uca.fr

organic solvents, leading to its use in numerous applications [3]. However, despite this interest and the availability of associated thermodynamic data [3-7], the potential of the (CO_2–E-LAC) mixture has never been evaluated for absorption refrigeration applications, which is the main motivation for this study. This work therefore goes beyond a simple preselection of solvents compatible with CO_2 and aims to evaluate the performance of a single-stage absorption refrigeration cycle using ethyl lactate as a potential absorbent. To this end, the model parameters of an equation of state (EOS) were determined using available thermodynamic properties of interest for a VAR cycle on (CO_2–E-LAC) system [3-7]. New excess enthalpy data were measured at a temperature lower than 298.15 K using a flow calorimetric technic developed in our laboratory. Finally, a comprehensive thermodynamic analysis, based on the simulation of an absorption refrigeration system, is presented to evaluate the real potential of this mixture for this application.

2. Thermodynamic Framework

To model with accuracy simultaneously enthalpy of mixing and vapor-liquid equilibria data we used an equation of state with complex mixing rules. This model, based on a φ-φ approach, was then used in this study to calculate the enthalpy and the vapor-liquid equilibria required to model the single stage absorption chiller.

2.1. Model description

In this work the equation of state Peng-Robinson [8] for mixture was used with MHV1 complex mixing rules [9]:

$$P = \frac{RT}{v-b_m} - \frac{a_m}{v^2+2b_m v-b^2} \tag{1}$$

$$\frac{a_m}{b_m RT} = \sum_i x_i \frac{a_i}{b_i RT} + \frac{\frac{g^{E,\gamma}}{RT} - \sum_i x_i \ln\left(\frac{b_i}{b_m}\right)}{q_1} \tag{2}$$

With q_1 an EOS dependent numerical constant (q_1 = 0.534). The components parameters a_i and b_i are calculated as follows:

$$a_i = a_{c,i} \cdot \alpha_i(T) \tag{3}$$

With:

$$a_{c,i} = 0.45724 \frac{R^2 T_{c,i}^2}{P_{c,i}} \tag{4}$$

And $\alpha_i(T)$, the Boston-Mathias alpha function [10] defined as follows:

$$For\ T < T_{c,i} : \alpha_i(T) = \left[1 + \left(0.37464 + 1.54226\omega_i - 0.26992\omega_i^2\right)\left(1 - \left(\frac{T}{T_{c,i}}\right)^{1/2}\right)\right]^2 \tag{5}$$

With:

$$m = 0.37464 + 1.54226\omega_i - 0.26992\omega_i^2 \tag{6}$$

$$For\ T > T_{c,i} : \alpha_i(T) = \left[exp\left(c\left(1 - \left(\frac{T}{T_c}\right)^d\right)\right)\right]^2 \tag{7}$$

With:

$$d = 1 + \frac{m}{2} \qquad \text{and} \quad c = 1 - \frac{1}{d} \tag{8}$$

$$b_i = 0.07780 \frac{RT_{c,i}}{P_{c,i}} \tag{9}$$

$$b_m = \sum_i x_i b_i \tag{10}$$

ω_i, $P_{c,i}$ and $T_{c,i}$ are the the acentric factor, the critical pressure and temperature of component *i* respectively and are given in Table 1.

Table 1. Characteristic parameters of pure compounds [10]

i	T_c /K	P_c /MPa	ω
CO_2	304.21	7.383	0.22362
E-LAC	796.26	6.26	0.36

The excess free enthalpy is calculated using NRTL activity coefficient model [11]:

$$\frac{g^{E,\gamma}}{RT} = x_1 x_2 \left(\frac{\tau_{21} G_{21}}{x_1 + x_2 G_{21}} + \frac{\tau_{12} G_{12}}{x_2 + x_1 G_{12}} \right) \tag{11}$$

$$\tau_{ij} = \frac{g_{ij} - g_{jj}}{RT} \qquad \textit{and} \qquad G_{ij} = exp\left(-\alpha \tau_{ij}\right) \tag{12}$$

And:

$$g_{ij} - g_{jj} = b_{ij}^{(0)} + b_{ij}^{(1)} (T - T_0) \tag{13}$$

τ_{ij}, G_{ij}, g_{ij}, $b_{ij}^{(0)}$and $b_{ij}^{(1)}$are NRTL interaction parameters. α is the non-random parameter and is set to 0.3. T_0 is equal to 273.15 K. For binary systems we have thus four binary ($b_{ij}^{(0)}$and $b_{ij}^{(1)}$) interaction parameters to adjust using experimental enthalpy and vapor liquid equilibria data.

2.2. Vapor-liquid equilibrium calculation

The physical equilibria that take place are expressed as follows:

$$CO_2^{(l)} \rightleftharpoons CO_2^{(v)} \tag{14}$$

$$\text{E-LAC}^{(l)} \rightleftharpoons \text{E-LAC}^{(v)} \tag{15}$$

To model these equilibria, a φ-φ approach [8] is employed and the phase equilibrium condition at a temperature T and a pressure p for CO2(1) and E-LAC(2) yields:

$$x_1 \phi_1^l(T, p, x_1) = y_1 \phi_1^v(T, p, y_1) \tag{16}$$

$$x_2 \phi_2^l(T, p, x_2) = y_2 \phi_2^v(T, p, y_2) \tag{17}$$

xi and yi are the mole fraction in the liquid and vapor phase respectively. ϕi is the fugacity coefficient in the liquid or vapor phase and is calculated as follows:

$$RTln(\phi_i) = \int_0^P \left(\overline{v_i} - \frac{RT}{P} \right) dP \tag{18}$$

$\bar{v}_i$ is the partial molar volume of constituent I and R is the universal gas constant. The *VLE* of (CO2–E-LAC) system are obtained by solving the two equilibrium equations (Eqs. 13 and 14) with respect to two unknowns using an iterative method. The composition at equilibrium of the liquid and vapor phase are calculated for a given temperature and pressure.

2.3. Enthalpy of mixing calculation

The excess molar enthalpy H^E of (CO_2–E-LAC) system is obtained from the *P-v-T* relationship in the mixture and for pure components following equations 19-21:

$$H^E(T,P,x) = H^R(T,P,x) - \sum_{i=1}^{n} x_i H_i^R(T,P) \quad (19)$$

$$H^R(T,P,x) = \int_{\infty}^{v} \left[T\left(\frac{\partial P}{\partial T}\right)_{v,x} - P \right] dv + Pv - RT \quad (20)$$

$$H_i^R(T,P) = \int_{\infty}^{v_i} \left[T\left(\frac{\partial P}{\partial T}\right)_{v_i} - P \right] dv_i + Pv_i - RT \quad (21)$$

$H^R(T,P,x)$ is the residual enthalpy of the mixture for a given temperature, pressure and composition and $H_i^R(T,P)$ is the residual enthalpy for pure component i, in the same temperature and pressure.

3. Experimental Thermodynamic

The enthalpies of mixing of CO_2 and ethyl-lactate were measured at 283.15 and pressure from 7 to 12 MPa on a large range of composition (xCO_2 = 0.1 to 0.95). For that purpose, a flow calorimetric technique developed in our laboratory was used.

Ethyl-lactate was purchased from Tokyo Chemical Industry with a purity > 99 % and was used without further purification. Carbon dioxide (purity of 99.995 %) was obtained from Air Products.

The calorimetric technique is described in detail in Coulier *et al.* work [12]. Briefly, enthalpy of mixing was determined in flow mode, using a Calvet type calorimeter. The overall experimental arrangement and the technical modifications made on the calorimeter to allow measurements at sub-ambient temperatures are described in [13]. Experiments are performed at constant temperature (±0.03 K). Carbon dioxide and E-LAC flow to a mixing cell unit located inside the calorimeter, where the heat released by the mixing process is obtained from thermopile signal. The pure fluids are supplied by two high-pressure syringe pumps (model 260DM from ISCO). These two pumps are regulated at a constant temperature (±0.1 K) using a thermostatic bath. The pressure is maintained constant during the experiments using two buffer volumes and a microvalve located at the end of the flow line. The pressure is measured by an electronic Keller pressure gauge placed at the outlets of the mixing cell with an uncertainty of 0.01 MPa.

The molar enthalpy of mixing ($\Delta_{mix}H$) is defined as a heat of mixing per mol of mixture (E-LAC and CO_2). In case where pure species and their related mixtures are in the same aggregation state at given temperature and pressure (liquid state in the present case), enthalpy changes on mixing are strictly equal to excess enthalpies (H^E). Thus, the terms “excess enthalpy” will be used thereafter to designate the measured data. This enthalpy is obtained from the calorimetric signal, detected by the thermopile surrounding the mixing cell as follows:

$$\Delta_{mix}H = H^E = \frac{\Delta signal}{K \cdot (\dot{n}_{CO_2} + \dot{n}_{E-LAC})} \quad (22)$$

where $\Delta signal$ is the difference between the electrical signal (mV) recorded during mixing and a baseline. The baseline signal is obtained when only E-LAC is flowing through the set up. K is a calibration constant used to convert the calorimetric signal, $\Delta signal$ (mV) into heat flux (mW). The calibration constant was determined at each temperature investigated in this study by measuring the heat of mixing of reference systems. $\dot{n}_{CO_2}$ and $\dot{n}_{E-LAC}$ are the molar flowrates. The experiments are performed at constant temperature and pressure and different gas-solvent flow rate fractions. Considering the uncertainties of fluid flow rates, thermopile calibration and calorimetric signal noises, the relative uncertainty on molar flow rates and molar enthalpies of mixing are less than 1.5% and 5 % respectively.

4. Simulation of the Absorption Refrigeration Cycle

The vapor absorption refrigeration cycle as illustrated in Figure 1 is made of a condenser, a refrigerant expansion valve (REV) an evaporator, an absorber, a circulation pump, a solution heat exchanger (SHX), a solution expansion valve (SEV) and a generator. The connecting lines between components are marked by numbered state points indicating the progression of the working fluids through the cycle.

In this cycle, the refrigerant (i.e., carbon dioxide) exits the evaporator as a low-pressure vapor. Arriving to the absorber, this vapor is absorbed by the diluted solution, which releases heat ($\dot{Q}_a$). The resulting mixture, known as concentrated solution, is pressurized by the pump and sent to the generator, where external heat ($\dot{Q}_g$) separates the CO_2 at high-pressure. The created vapor proceeds to the condenser, while the resulting diluted solution returns to the absorber at low pressure via the solution expansion valve, completing the solution cycle. To improve the chiller's efficiency, a SHX is placed before the generator, allowing the returning hot diluted solution to preheat the concentrated solution, enabling internal heat recovery. In the condenser, the CO_2 is condensed to high-pressure liquid refrigerant while releasing heat ($\dot{Q}_c$). The liquid CO_2 then passes through the refrigerant expansion valve and into the evaporator, where it evaporates, absorbing heat ($\dot{Q}_e$) from the external environment to complete the refrigerant cycle.

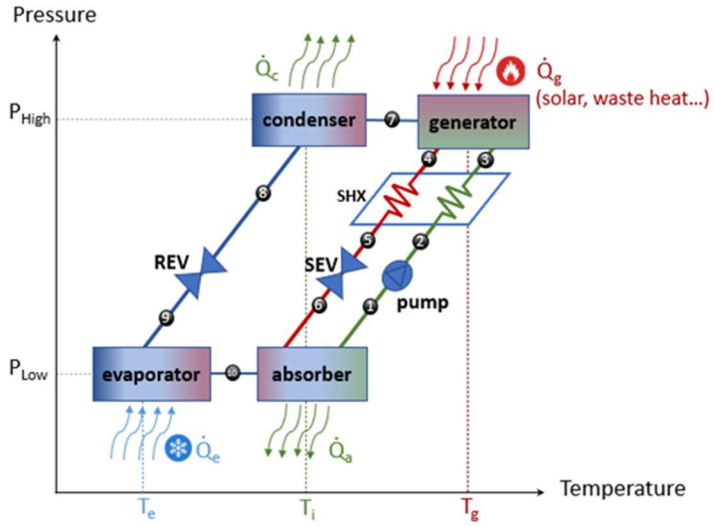

Figure 1: Schematic representation of the studied configuration of a single-stage absorption cycle

4.1. Modeling Assumptions

For the sake of simplicity, the following assumption were chosen:

- Steady state for all fluid streams.
- Negligible pressure drops. Thus, only two pressure levels exist in this cycle, $p_{Low} = p_1 = p_6 = p_9 = p_{10}$ and $p_{High} = p_2 = p_3 = p_4 = p_5 = p_7 = p_8$.
- Negligible heat losses to the surroundings.
- The condenser and the absorber are cooled by the same fluid and thus $T_i = T_a = T_c$.
- The solution at the outlet of the sorption elements is in equilibrium conditions.
- The refrigerant leaving the condenser and evaporator is in saturated conditions.
- $\varepsilon_{SHX} = 0.8$ and ideal heat exchangers for the rest of the components.
- Vapor leaving generator has zero absorbent content.
- The vapor leaving the generator is assumed to be in equilibrium with the concentration of the incoming liquid solution stream. Thus $T_7 = T^{sat}(w_3, p_7)$.
- Isentropic pumping.

4.2. Mass and Energy Balances

The simulation of the process consists of solving the mass and energy balances for an absorption chiller with a cooling capacity of 10 kW. As the working fluid is a binary mixture, the mass balance is described by

an overall mass balance and an absorbent mass balance for each component of the process as it is described in Eqs. (23-24). The used energy balance for each component is given by Eq. (25).

$$\sum \dot{m}_i = \sum \dot{m}_o \tag{23}$$

$$\sum(\dot{m}_i\, w_i) = \sum(\dot{m}_o\, w_o) \tag{24}$$

$$\sum((\dot{m}_i\, h_i) - (\dot{m}_o\, h_o)) + \sum \dot{W} + \sum \dot{Q}_{i/o} = 0 \tag{25}$$

$\dot{m}$, w and h represent respectively the mass flow rate (kg s^{-1}) the mass fraction of the absorbent and the specific enthalpy (kJ kg^{-1}) of the inlet (index i) and the outlet (index o) stream for the selected cycle component.

By expressing the mass and energy balances for each component of the cycle, and given that the fluid living the generator is considered pure refrigerant ($w_7 = 0$) and that the mass fractions and mass flow rates remain unchanged in the single-inlet and single-outlet process components (i.e., all components except the absorber and generator), the problem can be reduced to determining two main mass fractions ($w_1$and w_4), three mass flow rates ($\dot{m}_1$, $\dot{m}_4$ and $\dot{m}_7$) and the specific enthalpies at each point in the cycle.

To be able to solve the mass and energy balances two other equations were added for (1) the solution heat exchanger heat transfer and (2) the pump model.

(1) The solution heat exchanger effectiveness is given as the ratio of real heat transfer rate to maximum achievable heat transfer rate. The latter is calculated by multiplying the minimum capacitance rate by the temperature difference between the inlet streams (T_2 and T_4). Since, in our study, the hot stream has the minimum capacitance rate, the effectiveness of the SHX can be written as in Eq. (26).

$$\varepsilon_{SHX} = \frac{T_4 - T_5}{T_4 - T_2} \tag{26}$$

(2) In this work, a standard pump model for an incompressible fluid, based on the principle of an isentropic pressure change was used with 100% efficiency:

$$\dot{W} = \frac{\dot{m}_1\, v_1\, (p_{high} - p_{low})}{\eta_{pump}} \tag{27}$$

v_1 and η_{pump} are the solution's specific volume at the pump inlet ($m^3.kg^{-1}$) and pump efficiency, respectively.

4.3. Nominal Conditions

For this study, the output temperatures of each corner component in the process are used as inputs. These inputs are fixed to nominal conditions summarized in Table 2.

Table 2. Nominal operating conditions

Component	Defined temperature
Absorber	$T_1 = T_i = 298.15$ K
Generator	$T_4 = T_g = 363.15$ K
Condenser	$T_8 = T_i = 298.15$ K
Evaporator	$T_{10} = T_e = 278.15$ K

The temperatures T_8 and T_{10} define the two pressure levels in the system using the properties of pure carbon dioxide. In fact, the high pressure is set by the condenser outlet saturation conditions (state 8): $p_{High} = p^{sat}$ (T_8, w_8) and the low pressure is set by the evaporator outlet saturation conditions (state 10): $p_{Low} = p^{sat}$ (T_{10}, w_{10}).

Using the two other temperatures (T_1 and T_4), the mass fractions at points 1 and 4 can be determined based on the assumption of equilibrium states at these points. Thus, the mass fractions of the solutions leaving the absorber (w_1) and the generator (w_4) can be calculated as follows: $w_1 = w^{sat}$ (T_1, p_{Low}) and $w_4 = w^{sat}$ (T_4, p_{High}).

These pressures (p_{High} and p_{Low}) and mass fractions (w_1 and w_4), as well as the other thermodynamic properties required for process modeling (other temperatures and specific enthalpies), are first calculated with

the thermodynamic model developed in this study, using ProSim's Simulis Thermodynamics software, integrated into Excel.

In order to solve the mass and energy balances of the absorption refrigeration cycle, the mass flow rate $\dot{m}_1$, chosen as an input, is initially set at 1 kg.s^{-1} and a sequential calculation procedure, in which the balance equations are solved in order, is used. The mass and energy flows are thus determined successively from the previously known thermodynamic states, without the use of a nonlinear solver. Once the mass and energy balances have been completely established, the results are normalized proportionally in order to obtain a cooling capacity of 10 kW. The consistency of the results is finally verified by the residuals of the global mass and energy balances.

5. Results and discussion

5.1. Modeling results

Binary interaction parameters have been determined using *VLE* and excess enthalpy data from the literature [3-7] and determined in this work. Table 3 presents the number of data used for parameters adjustment, the temperature and pressure conditions, as well as the absolute average relative deviation (AARD%) used to evaluate model quality for each property.

Table 3. Experimental VLE and enthalpy data from the literature and their comparison with correlation results from the model.

N[a]	T (K)	p^{max} (MPa)	*AARD* (%)[b]
	Vapor-liquid-equilibria		
65	313-393	12.64	8.8
	Excess enthalpy		
165	283-303	12	11.5

[a] N = number of experimental data points.
[b] $AARD = 1/N \sum_i^N \left|X_i^{\exp} - X_i^{\text{calc}}\right| / X_i^{\exp}$ with $X = x_{CO2}$ or H^E

The adjustment of the BIPs of the model (Eq. (10)) was performed with Minuit software, using Simplex method and the objective function F as expressed in Eq. (25):

$$F = \frac{w_{VLE}}{n_{VLE}} \sum_i^{n_{VLE}} \left(\frac{x_{CO_2,i}^{exp} - x_{CO_2,i}^{calc}}{u(x_{CO_2,i}^{exp})} \right)^2 + \frac{w_H}{n_H} \sum_i^{n_H} \left(\frac{H_i^{E,exp} - H_i^{E,calc}}{u(H_i^{E,exp})} \right)^2 \quad (28)$$

Where $x_{\mathrm{CO_2},i}^{\exp}$, $x_{\mathrm{CO_2},i}^{\text{calc}}$, $H_i^{\mathrm{E,exp}}$ and $H_i^{\mathrm{E,calc}}$ are the experimental and calculated CO_2 molar fraction and excess enthalpy of data i; n_{VLE} and n_H are the number of experimental vapor liquid equilibria and enthalpy data points respectively and w denotes weighting factors. As model parameters are much more sensitive to *VLE* data than to H^E data, weighting factors were initially set to $w_{VLE} = 1$ and $w_H = 0.25$ and then, manually adjusted to ensure the best compromise between the reproduction of *VLE* and H^E data. The resulting BIPSs are given in Table 4 and the correlation of the excess enthalpies is illustrated in figure 2.

Table 4. BIPs of the EOS (Eq. (13))

Constituent	$b_{ij}^{(0)}$	$b_{ij}^{(1)}$
CO_2–E-LAC	2090.7	12.409
E-LAC-CO_2	-1260.2	-3.5168

5.2. Experimental results

The excess molar enthalpies of the (CO_2–E-LAC) system as a function of the CO_2 molar fraction were determined at 283.15 K and under pressure from (7.00 to 12.00) MPa. The experimental data are represented in Figure 2. Exothermic excess enthalpies were observed for each temperature and pressure condition. For a given mole fraction and at 283.15 K, mixing enthalpies are slightly less exothermic as the pressure increases.

And for a given mole fraction and at 7.00 MPa, mixing enthalpies are more exothermic as the temperature increases.

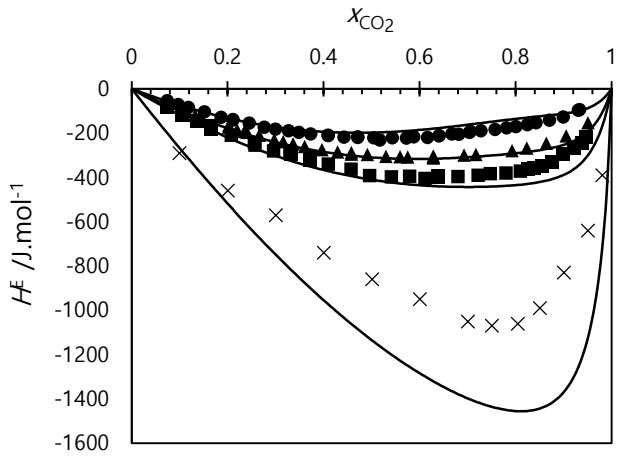

Figure 2: Experimental excess molar enthalpies for (CO_2–E-LAC) sytem. Experimental data at 283.15 K, ■ 7.00 MPa; ▲ 9.00 MPa; ● 12.00 MPa and × at 298.15 K and 7,00 MPa [3]. — PR EOS with MHV1 mixing rules.

5.3. Performance evaluation of the vapor absorption cycle

The cycle performance analysis was carried out using various performance indicators, namely:

- Overall coefficient of performance:

$$COP_{overall} = \dot{Q}_e/(\dot{Q}_g + \dot{W}) \tag{29}$$

- Thermal coefficient of performance:

$$COP_{th} = \dot{Q}_e/\dot{Q}_g \tag{29}$$

- Electrical coefficient of performance:

$$COP_{elec} = \dot{Q}_e/\dot{W} \tag{29}$$

- Circulation ratio:

$$f = \frac{\dot{m}_{concentrated\ solution}}{\dot{m}_{refrigerant}} \tag{29}$$

- Concentration difference between concentrated and diluted solutions:

$$\Delta w = w_4 - w_1 \tag{29}$$

Simulation results for the absorption refrigeration process using the (CO_2–E-LAC) working fluid pair were compared with those for traditional (NH_3–H_2O) and (H_2O–LiBr) chillers simulated with Engineering Equation Solver software. Given that these systems operate at different pressure and temperature ranges, this comparison isn't meant to suggest a direct industrial replacement, but rather to show how (CO_2–E-LAC) performs compared to traditional cycles. To ensure a consistent comparison, performance was evaluated for a cooling capacity of 10 kW and identical operating temperatures (T_1, T_4, T_8 and T_{10}), regardless of the working pressures specific to each system.

5.3.1. Results under nominal operating conditions

Simulation results for the absorption refrigeration process under nominal operating conditions and for a cooling capacity of 10 kW are summarized in the Table 5 for the three studied working fluid.

Table 5. Simulation results of absorption chiller using (CO_2–E-LAC), (NH_3–H_2O) or (H_2O–LiBr) under nominal conditions

Working fluid pair	CO_2–E-LAC	NH_3–H_2O	H_2O–LiBr
$COP_{overall}$	0.36	0.72	0.84
COP_{th}	0.37	0.72	0.84
COP_{elec}	10.93	7.0E+02	4.6E+05
$\dot{Q}_{\mathrm{g}}$ (kW)	26.74	13.92	11.90
f	5.60	2.53	3.43
Δw	0.14	0.25	0.20
$\dot{W}$ (kW)	0.91	1.3E-02	2.2E-05
P_{High} (MPa)	6.45	1.00	0.0030
P_{Low} (MPa)	4.00	0.51	0.0009

Table 5 shows that the COP_{th} of the absorption chiller using the (CO_2–E-LAC) fluid pair is about 0.37 which is lower compared to chillers operating with NH_3–H_2O and H_2O–LiBr. This difference in our system is mainly due to the higher fluid circulation rates, which increase the heat input to the generator. These flow rates depend, in turn, on the concentration difference (Δw) and on the refrigerant's vaporization enthalpy. Indeed, since our system (CO_2–E-LAC) has a lower Δw than the two others, a higher solution flow rate is required to maintain the same refrigerant flow rate. We can also observe that the COP_{elec} for (CO_2–E-LAC) chiller is one to four orders of magnitude lower than that of chillers operating with (NH_3–H_2O) and (H_2O–LiBr) respectively. This is due to the significantly higher $\dot{W}$ for our system, due to a greater pump inlet-outlet pressure difference between all three systems.

Despite the lower performance of the (CO_2–E-LAC) cycle compared with traditional working fluid pairs, it must be emphasized that the key advantage of using (CO_2–E-LAC) is avoiding the technical problems related to traditional pairs, such as toxicity, corrosion, crystallization or the need for a rectifier. In addition, the performance of the (CO_2–E-LAC) cycle can be improved by modifying the cycle's operating conditions, as discussed in the next section.

5.3.2. Parametric analysis

- Evaporator temperature

One advantage of using (CO_2–E-LAC) as working fluid pair is the ability to produce cooling at negative temperatures. However, the analysis showed that lowering this temperature to 268.15 K yield to a drop in COP_{th} down to 0.26. For this reason, (CO_2–E-LAC) mixture is not suitable for producing deep freezing, but rather for air-conditioning applications or use at temperatures close to 273.15 K. On the other hand, increasing T_{e} from 278.15 K to 288.15 K increased the COP_{th} up to 0.45 as shown in Figure 3. The same figure illustrates an improvement in COP_{elec} with increasing T_{e}. This is due to the reduction in pump power following the reduction in solution flow rate and the pressure difference between the absorber and the generator. These improvements can be explained by the fact that the increase in evaporator temperature raises the evaporator and the absorber pressure, which enhances the CO_2 absorption and thus increases Δw (Figure 3). Higher solubility in the absorber means less solution flow rate to produce the same amount of refrigerant. So, for the same cooling capacity, less solution flow fed to the generator and a reduction of the energy duties is achieved. Figure 3 shows that f decreases with increasing T_{e}.

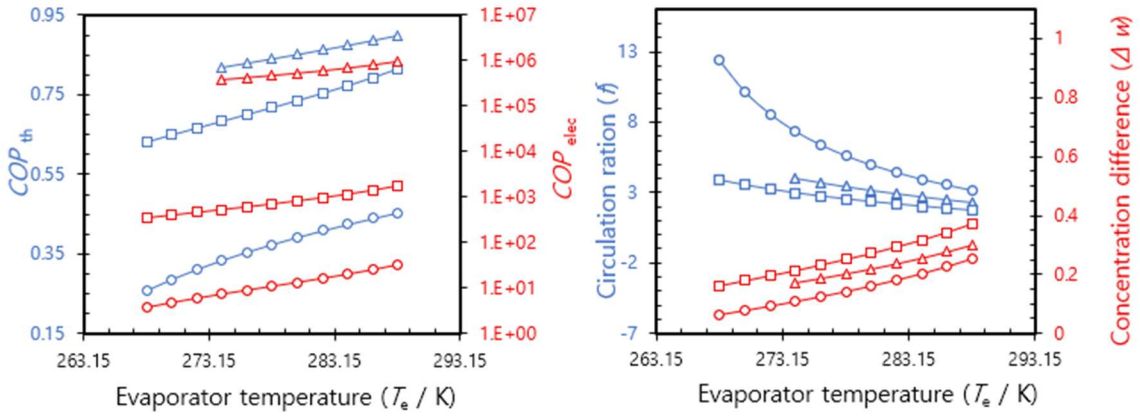

Figure 3: Calculated COP, f ratio and Δw vs evaporator temperature for: ○ CO_2–E-LAC; □ NH_3-H_2O and △ H2O-LiBr systems

- Intermediate temperature

The influence of the intermediate temperature on the performance of the system is illustrated in Figure 4. Reducing T_i, down to 293.15 K, results in an improvement of COP_{th}, raising it to 0.48. This is because a decrease in this temperature, yield both to an increase in CO_2 absorption at the absorber, and to a decrease in condenser pressure, and consequently, in the generator. This pressure drop at a same generator temperature promotes the desorption of more CO_2. These two phenomena increase the Δw (Figure 4), which leads to a reduction in the f and therefore a decrease in solution flowrates and energy duties.

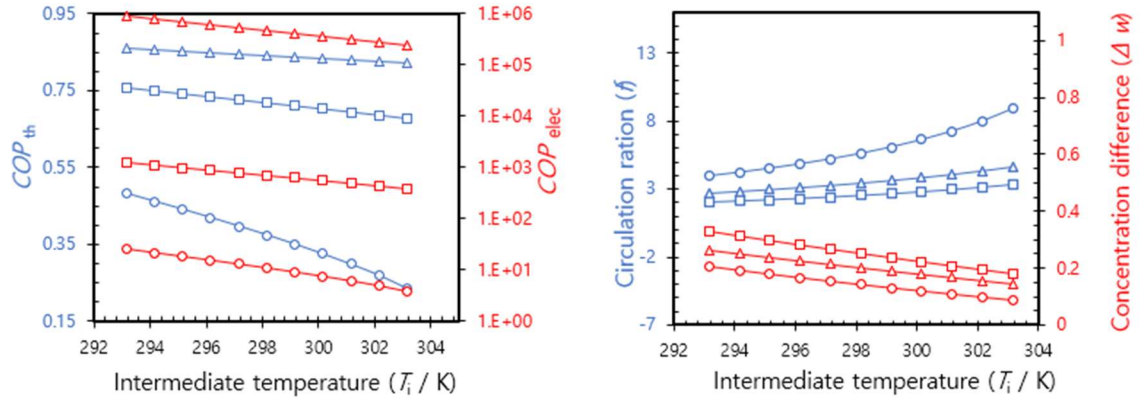

Figure 4: Calculated COP, f ratio and Δw vs intermediate temperature for: ○ CO_2–E-LAC; □ NH_3-H_2O and △ H_2O-LiBr systems

- Generator temperature

The influence of generator temperature on cycle performance was studied by varying T_g between 343.15 K and 383.15K. For the COP_{th}, this analysis was extended to 320 K to determine the minimum temperature required to start the desorption of the refrigerant from the absorbent (cut-off temperature). As shown in Figure 5, this cut-off temperature for CO_2–E-LAC is slightly higher than those of traditional working fluid pairs. This figure reveals also that for all three studied working fluid pairs, increasing T_g results in a significant increase in COP_{th} up to an optimum temperature after which it stabilizes with a slight decrease. The optimum temperatures (355.15, 339.15 and 331.15K for CO_2–E-LAC, NH_3-H_2O and H_2O-LiBr respectively) are relatively low, enabling the use of low-temperature heat sources. Increasing T_g improves the COP_{elec} (Figure 5) and the circulation ratio f (Figure 5). Indeed, a higher T_g promotes refrigerant desorption, which increases Δw (Figure 5), leading to a reduction in solution flowrate, and therefore a reduction in pump power. As a conclusion, increasing the generator temperature reduces the circulation ratio but does not improve the COP for the three systems.

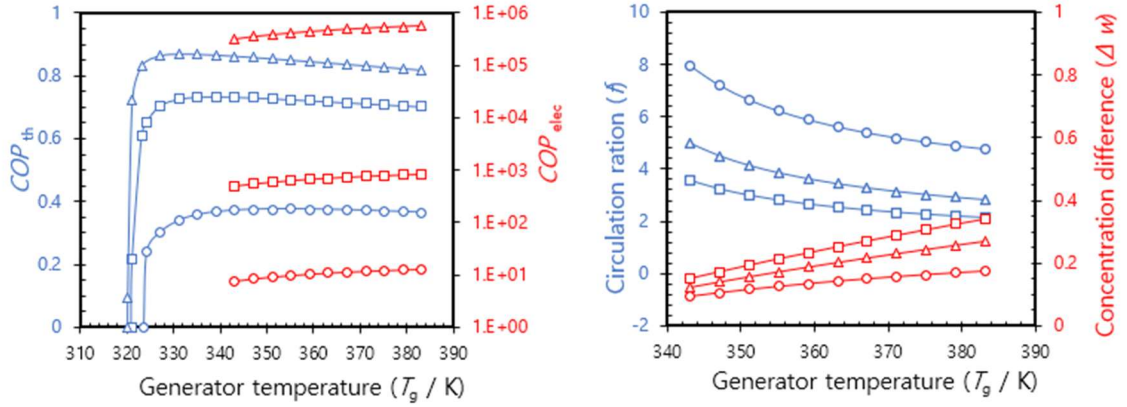

Figure 5: Calculated COP, f ratio and Δw vs generator temperature for: ○ CO_2–E-LAC; □ NH_3-H_2O and △ H_2O-LiBr systems

6. Conclusions

A thermodynamic characteristic (CO_2–E-LAC) working fluid was performed to analyze the performance of a vapor absorption cycle using this WF pair. To achieve this task the binary interaction parameters of Peng-Robinson equation of state using MHV1 mixing rule with NRTL activity coefficient model were determined. These BIPs were adjusted using available vapor-liquid-equilibria and enthalpy data. Finally, this equation of state was used to model a vapor absorption chiller and analyze the influence of the operating parameters. A COP of 0.36 was found at the nominal condition investigated. Despite the poorer performance of the (CO_2–E-LAC) cycle compared to traditional working fluid pairs, it should be emphasized that the main advantage of using (CO_2–E-LAC) is to avoid the technical issues associated with conventional pairs utilization, such as toxicity, corrosion, crystallization or the need of a rectifier.

7. Nomenclature

a	attractive term of EOS (Pa× m^6×mol^{-2})	b	repulsive term of EOS (m^3×mol^{-1})
b	NRTL interaction parameter	COP	coefficient of performance
F	objective function	f	circulation ratio
G g,	NRTL interaction parameter	$g^{E,\gamma}$	excess Gibbs energy
h	specific enthalpy (kJ×kg^{-1})	H	molar enthalpy (J×mol^{-1})
K	calibration constant ($V.W^{-1}$)	$\dot{m}$	mass flowrate (kg×s^{-1})
$\dot{n}$	molar flowrate (mol×s^{-1})	p	pressure (Pa)
$\dot{Q}$	Heat flow (W)	q_1	MHV1 constant
R	molar gas constant (8.314472 J×mol^{-1}×K^{-1})	T	temperature (K)
v	molar volume (m^3×mol^{-1})	w	mass fraction
$\dot{W}$	pump work	x	molar fraction
y	vapor molar fraction	α	EOS alpha function
α	NRTL non-randomness parameter	ε_{SHX}	solution heat exchanger effectiveness
η	pump efficiency	ϕ	fugacity coefficient
τ	NRTL interaction parameter	ω	acentric factor

Acknowledgements

This work was realized with the financial support of region Auvergne-Rhône-Alpes through an international collaborative project (Ambition International).

References

[1] Altamirano A, Pierrès N, Stutz, B. Review of small-capacity single stage continuous absorption system operating on binary working fluids for cooling: Theoritical, experimental and commercial cyles. *Int J Refrig* 2019;**106**,350-373.

[2] Kerleaux M., Rodier L., Andanson J-M., Dequidt A., Coulier Y., 2022. "Natural Working Fluids for Absorption Refrigeration," 15th IIR-Gustav Lorentzen Conference on Natural Refrigerants. Trondheim, Norway, paper #0223.

[3] Matsuda, H, Furukawa Y, Fukui T, Kurihara K, Tochigi K, Ochi K. Excess molar enthalpies in the binary system of carbon dioxide + ethyl lactate at 298.15 and 303.15 K and 5.0–7.0 MPa. *Fluid Phase Equilib* 2023;**572**:113838.

[4] Behera, US, Shim J, Lee HS, Byunet H-S. Solution Thermodynamics of Methyl, Ethyl, Propyl, and Butyl Lactates in High-Pressure CO_2. *ACS Omega* 2025;**10**:35230-35240.

[5] Cho, DW, Shin MS, Shin J, Bae W, Kim H. High-Pressure Phase Behavior of Methyl Lactate and Ethyl Lactate in Supercritical Carbon Dioxide. *J. Chem Eng Data* 2011;**56**:3561-3566.

[6] Paninho AB, Nunes AVM, Paiva A, Najdanovic-Visak V. High pressure phase behavior of the binary system (ethyl lactate+carbon dioxide), *Fluid Phase Equilib* 2013;**360**:129-133.

[7] Villanueva Bermejo D, Ibáñez E, Stateva RP, Fornari T. Solubility of CO_2 in Ethyl Lactate and Modeling of the Phase Behavior of the CO_2 + Ethyl Lactate Mixture. *J Chem Eng Data* 2013;**58**:301-306.

[8] Peng D-Y, Robinson DB. A New Two-Constant Equation of State. *Ind Eng Chemistry Res* 1976;**15**:59-64.

[9] Huron M-J, Vidal J. New mixing rules in simple equations of state for representing vapour-liquid equilibria of strongly non-ideal mixtures. *Fluid Phase Equilib* 1979;**3**:255-271.

[10] Neau E, Hernández-Garduza O, Escandell J, Nicolas C, Raspo I. The Soave, Twu and Boston–Mathias alpha functions in cubic equations of state: Part I. Theoretical analysis of their variations according to temperature. *Fluid Phase Equilib* 2009;**276**:87-93.

[11] Renon H, Prausnitz JM, Local compositions in thermodynamic excess functions for liquid mixtures *AIChE J* 1968;**14**:135-144.

[12] CoulierY, Ballerat-Busserolles K, Mesones J, Lowe A, Coxam J-Y. Excess Molar Enthalpies and Heat Capacities of {2-Methylpiperidine–Water} and {N-Methylpiperidine–Water} Systems of Low to Moderate Amine Compositions. *J Chem. Eng Data* 2015;**60**:1563-1571.

[13] Ramírez-Ramos, GE, Zgar Y, Salavera D, Coulier Y, Ballerat-Busserolles K, Coronas A. *Fluid Phase Equilib* 2021;**532**:112915.